

12-22-2020

## Changes in the structure and properties of ZrO<sub>2</sub> detonation coatings during annealing

B. K. Rakhadilov

*Sarsen Amanzholov East Kazakhstan University; PlasmaScience LLP, Kazakhstan*

D. N. Kakimzhanov

*Sarsen Amanzholov East Kazakhstan University; D. Serikbayev East Kazakhstan Technical University, Kazakhstan*

G. Botabaeva

*Sarsen Amanzholov East Kazakhstan University, Kazakhstan*

D. B. Buitkenov

*Sarsen Amanzholov East Kazakhstan University; PlasmaScience LLP, Kazakhstan*

N. Kantai

*Sarsen Amanzholov East Kazakhstan University; D. Serikbayev East Kazakhstan Technical University, Kazakhstan*

*See next page for additional authors*

Follow this and additional works at: <https://www.ephys.kz/journal>

 Part of the [Materials Science and Engineering Commons](#), and the [Physics Commons](#)

### Recommended Citation

Rakhadilov, B. K.; Kakimzhanov, D. N.; Botabaeva, G.; Buitkenov, D. B.; Kantai, N.; and Bayatanova, L. B. (2020) "Changes in the structure and properties of ZrO<sub>2</sub> detonation coatings during annealing," *Eurasian Journal of Physics and Functional Materials*: Vol. 4: No. 4, Article 5.  
DOI: <https://doi.org/10.29317/ejpfm.2020040405>

This Original Study is brought to you for free and open access by Eurasian Journal of Physics and Functional Materials. It has been accepted for inclusion in Eurasian Journal of Physics and Functional Materials by an authorized editor of Eurasian Journal of Physics and Functional Materials.

---

## Changes in the structure and properties of ZrO<sub>2</sub> detonation coatings during annealing

### Authors

B. K. Rakhadilov, D. N. Kakimzhanov, G. Botabaeva, D. B. Buitkenov, N. Kantai, and L. B. Bayatanova

# Changes in the structure and properties of $ZrO_2$ detonation coatings during annealing

B.K. Rakhadilov<sup>\*,1,2</sup>, D.N. Kakimzhanov<sup>1,3</sup>, G. Botabaeva<sup>1</sup>,  
D.B. Buitkenov<sup>1,2</sup>, N. Kantai<sup>1,3</sup>, L.B. Bayatanova<sup>2,3</sup>

<sup>1</sup>Sarsen Amanzholov East Kazakhstan University, Ust-Kamenogorsk, Kazakhstan

<sup>2</sup>PlasmaScience LLP, Ust-Kamenogorsk, Kazakhstan

<sup>3</sup>D. Serikbayev East Kazakhstan Technical University, Ust-Kamenogorsk, Kazakhstan

E-mail: rakhadilovb@mail.ru

DOI: 10.29317/ejpfm.2020040405

Received: 20.10.2020 - after revision

The article studied the effect of annealing on the structure and properties of zirconium dioxide coatings obtained by detonation spraying. Detonation spraying was realized on a computerized detonation spraying complex of the new generation CCDS2000. Determined that coatings made of zirconium dioxide are characterized by high adhesive strength of adherence to the substrate. Thermal annealing of coated samples was performed at temperatures of 900-1200 ° C. It was determined that the microhardness of zirconium dioxide coatings increases by 10-25% depending on the annealing temperature after annealing. The results of nanoindentation showed that the nanohardness of the coatings after annealing at 1000 ° C increases by 50%. It was determined that after annealing at 1000 ° C, the elastic modulus of the coatings increases, which indicates a decrease in plasticity and an increase in the strength of the coatings. X-ray diffraction analysis showed that the phase composition of coatings before and after annealing consists of  $t-ZrO_2$ . After annealing occurs there is an increase in the degree of  $t-ZrO_2$  tetragonality. Electron microscopic analysis showed that an increase in the number and size of micro-continuity in the form of thin layers after annealing. Determined that increase the hardness of zirconium dioxide after annealing at 900-1200 ° C is associated with a higher degree of tetragonality  $t-ZrO_2$  phase.

**Keywords:** zirconium dioxide, coating, detonation spraying, hardness, annealing, microstructure, phase, indentation.

## Introduction

High-speed spraying methods can significantly expand the capabilities of traditional thermal spraying coatings used to protect parts from wear and corrosion [1-4]. Gas-thermal high-speed methods for producing coatings include methods of detonation [5], high velocity air-gas plasma (HVAGP) [6] and high velocity oxygen-fuel coating (HVOF) spraying [7]. Among them, the most promising is detonation spraying. Detonation spraying is one of the methods of thermal spraying of coatings, which is carried out using a special detonation gun filled with explosive gas mixture. A powdery spray material is used to form a coating. In the process of detonation, the particles of the powder are accelerated to high speeds (up to 1000 m/s), their melting and deposition on the sprayed surface [8].

The detonation method is promising for obtaining heat-resistant and heat-protective coatings on the blades of gas turbine engines due to the low porosity of the coatings and the saving of the chemical composition of the initial powder in the coatings, as well as the high adhesion strength of the coatings. Zirconium dioxide coatings are often used as upper thermal barrier layers of heat-protective coatings [9, 10]. There is very little work devoted to the study of zirconium dioxide obtained by detonation coatings. At the same time, detonation coatings allows one to obtain a set of properties necessary for heat-protective coatings: high adhesion of the coating, thickness up to 300  $\mu\text{m}$ , significant porosity, as well as the ability to adjust the structure and properties of the coating by selecting processing parameters. Therefore, the study of structural transformations in detonation coatings of zirconium dioxide during heat treatments is of great interest. This work is devoted to studying the impact of thermal annealing on the structure and hardness of zirconium dioxide coatings.

## Materials and methods of research

Detonation coatings were obtained on a computerized complex of new generation detonation spraying CCDS2000 (Computer Controlled Detonation Spraying), [11-14]. A general view and a schematic diagram of the detonation spraying process are presented in Figure 1. The channel inside the gun barrel is filled with gases using a high-precision gas distribution system, which is controlled by a computer. The process begins with filling the channel with carrier gas. After that, a certain portion of the explosive mixture is supplied in such a way that a layered gas medium is formed, consisting of an explosive charge and a carrier gas. Using a carrier gas stream, the powder is injected into the barrel (using a computer-controlled feeder) and forms a cloud. The substrate is placed at a certain distance from the exit from the trunk. After part of the powder is injected, the computer gives a signal to initiate detonation. This is realized using an electric spark. The duration of explosive combustion of a charge is about 1 ms. a detonation wave is formed in the explosive mixture, which in the carrier gas transforms into a shock wave. Detonation products (heated to 3500-4500 K) and carrier gas (heated by a shock wave to 1000-1500 K) move at a supersonic speed. The interaction time of

gases with the sprayed particles is 2-5 ms. Particle velocities can reach  $800 \text{ m s}^{-1}$  [15-18].

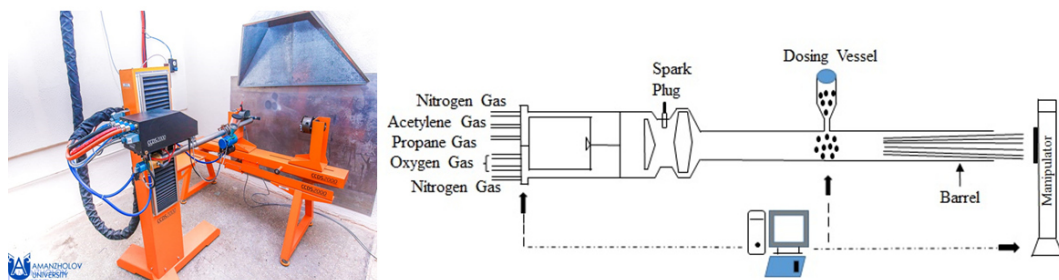


Figure 1. Computerized detonation complex CCDS2000 (a) and its circuit diagram (b).

Stainless steel 12X18H10T was chosen as a substrate. The samples were sandblasted before coating. A powder of zirconium dioxide stabilized with yttrium oxide was used to obtain coatings. The particle size of the powder was up to  $25\text{-}30 \mu\text{m}$ . Thermal annealing of the coated samples was carried out in a laboratory tube resistance furnace SUOL-0.4.4/12-M2-U4.2 in a vacuum of  $10^{-2}$  Pa at temperatures of  $900\text{-}1200^\circ\text{C}$  during 1 h. The temperature was measured and controlled by a VRT-2 precision thermoregulator using two thermocouples of the CCI 1378 type. The microstructure of the coatings was studied by metallographic analysis using a Neophot-21 microscope and scanning electron microscopy using JSM-6390LV and PhenomProX scanning electron microscopes. The microhardness of the samples was measured by the indentation method of a diamond indenter on a PMT-3 device in accordance with GOST 9450-76, at a load of 200 g and exposure under a load of 10 s. The phase composition of the samples was studied by X-ray diffraction analysis on an X'PertPro diffractometer using  $\text{CuK}\alpha$  radiation. The measurement of hardness and elastic modulus was determined by the indentation method on a «NanoScan - 4D compact» nanohardness meter in accordance with GOST R 8.748-2011 and ISO 14577 indentation with a load of 0.1 N.

## Research results and discussion

Adhesion is one of the main factors determining the quality of the coating. In Figure 2 shows testing the adhesive strength results of coatings by scratch testing. Registration various parameters during the testing process allow recording various stages of coating failure. So,  $L_{c1}$  indicates the moment when the first crack appears,  $L_{c2}$  - peeling of the coating sections,  $L_{c3}$  - plastic abrasion of the coating to the substrate [19]. Visible that  $\text{ZrO}_2$  coatings, the first crack is formed at load  $L_{c1} = 11.6 \text{ H}$ . Then the process continues with a certain cycle. The coating partial abrasion until substrate was judged by a sharp change in the intensity of the growth of the friction force. This happened at load  $L_{c3} = 29.65 \text{ H}$ . This significance  $L_{c3}$  said value indicates a high adhesion strength of the coatings to the substrate.

Figure 3 shows the dependences of the microhardness variation along the depth of the experiment sample before and after annealing at different temperatures. The maximum increase in microhardness is observed in samples after

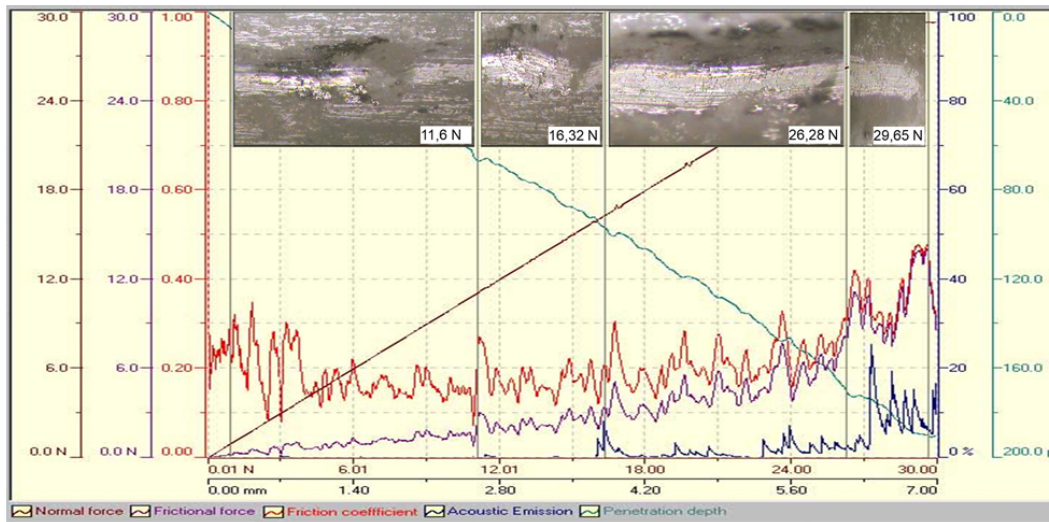


Figure 2. Results of the scratch test coatings made of zirconium dioxide.

annealing at 1000 °C. The maximum depth of the hardened layer for all coatings is 400 μm, i.e. corresponds to the thickness of the coating.

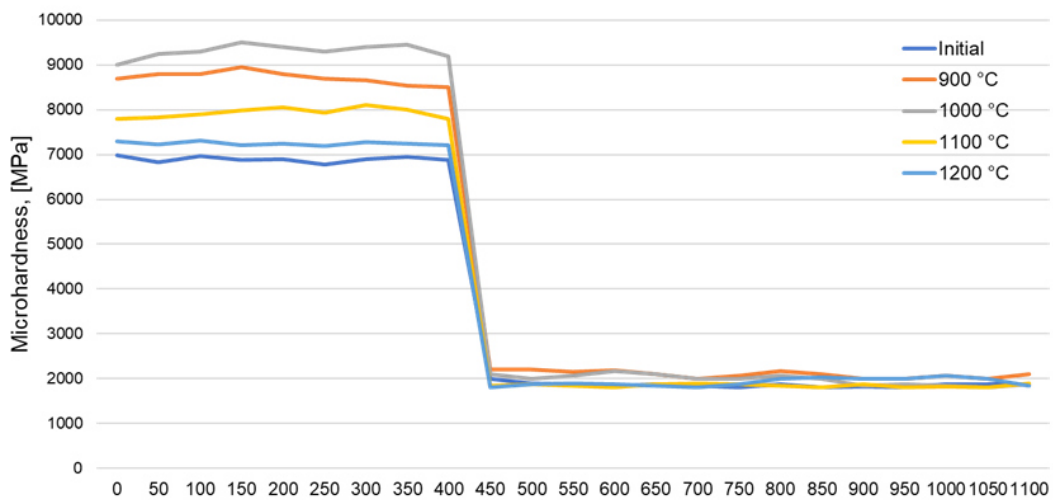


Figure 3. Microhardness of coatings from zirconium dioxide.

The region of thermal influence and the diffusion zone are not observed according to metallographic analysis and microhardness. This is due to the fact that during detonation sputtering the substrate heats up to only 200-300 °C, that the surface of the substrate does not undergo structural and phase transformations, and also during annealing the diffusion processes do not occur between the zirconium dioxide coating and the iron-based substrate at the indicated temperatures.

The modules of elasticity and nanohardness of the coatings were determined on the results of nanoindentation (Table 1). The results showed that the nanosolidity increases in comparison with the sample before and after annealing. In this case, the highest value of the nanohardness of 15.8 GPa is observed after annealing at 1000 °C. It can be seen that after annealing at 1000 °C, the elastic modulus of the coatings increases, which indicates a decrease in plasticity and an increase in the strength of the coatings.

Table 1.

The results of nanoindentation.

Coatings	Hanohardness, GPa	Young's modulus, GPa
ZrO <sub>2</sub> initial	9.9	176
ZrO <sub>2</sub> after annealing at 900°C	11.6	178
ZrO <sub>2</sub> after annealing at 1000°C	15.8	245
ZrO <sub>2</sub> after annealing at 1100°C	12.8	174
ZrO <sub>2</sub> after annealing at 1200°C	8.59	147

We can note a clear discrepancy (1.5 times) in the quantitative values of the results with good qualitative agreement by comparing the results of determining the hardness of the material at different loads on the indenter (microhardometry (Figure 3) and nanosolidometry (Table 1). This can be explained by the fact that during nanocontact interaction, due to the small (tens of nanometers) dimensions of the indent, the degree of imperfection of the material under the indent is significantly reduced, which helps to bring the behavior of real material closer to ideal [20].

Figure 4 shows the diffraction patterns of the coatings before and after annealing. The results of x-ray structural analysis of coatings showed that the coating in the initial and after annealing consists of the t-ZrO<sub>2</sub> phase. The diffractogram of samples after annealing differs from the diffractogram before annealing in that instead of single lines (211) and (222), the t-ZrO<sub>2</sub> phase gives double lines. Also, after annealing the pairs of closely spaced each other lines (002) - (110) and (004) - (103), the t-ZrO<sub>2</sub> phases are moved wider apart. All this is related an increase in the tetragonality of the t-ZrO<sub>2</sub> phase. So as known [21] that the distance between paired lines depends on the c/a ratio. The larger it is, i.e., the greater the degree of tetragonality, the paired lines are further apart each other. In turn, the degree of tetragonality depends linearly on the oxygen content of zirconium dioxide. In our case, an increase in the degree of tetragonality after annealing due to an increase in the oxygen content is quite possible, since the annealing of the samples was carried out in a low vacuum.

Based on x-ray diffraction analysis, it can be claimed that the increase in the hardness of zirconium dioxide after annealing is associated with an increase in the tetragonality of the t-ZrO<sub>2</sub> phase. Since the greater the degree of tetragonality of the tetragonal phase, the higher the strength of the material [22].

It can be seen on Figure 5 that thermal extraction at 1000 °C based on structural influence is not provided. However, an increase in the number and size of microcontinuities in the form of thin layers is observed. This helps to reduce internal stresses associated with operation. The formation of microcontinuities in the form of thin interlayers is the reason for the strong discrepancy in the data on the microhardness and nanosolidness of the coating.

Figure 6 shows SEM-images of coatings and the results of X-ray microanalysis. The coating has a classic structure characteristic of gas thermal spraying methods. The coating is characterized by the presence of high density and uniformity as well as the presence of individual pores. Two groups of pores can be distinguished: rounded micro-discontinuities several micrometers in size and

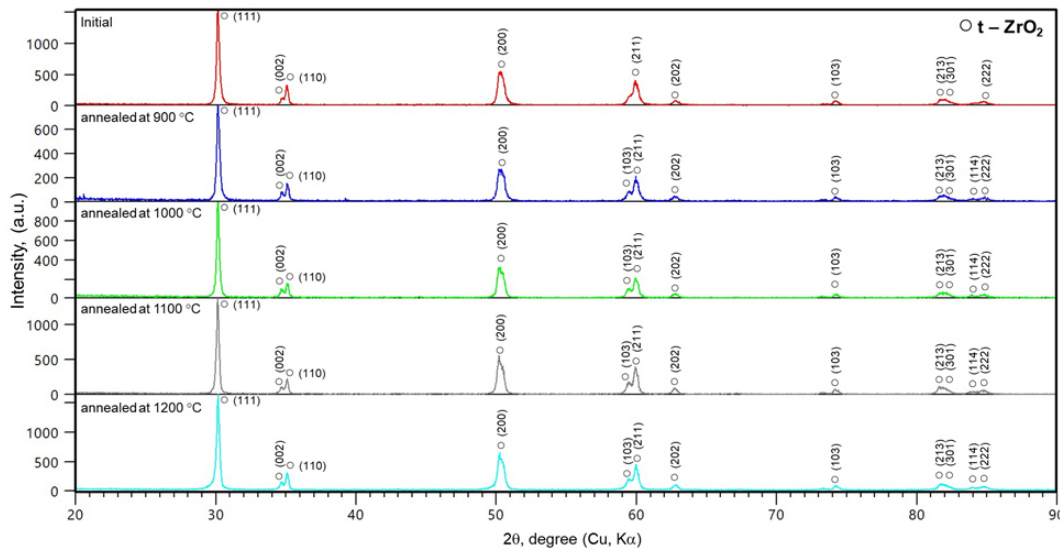


Figure 4. X-ray diffraction patterns of coatings from zirconium dioxide before and after annealing.

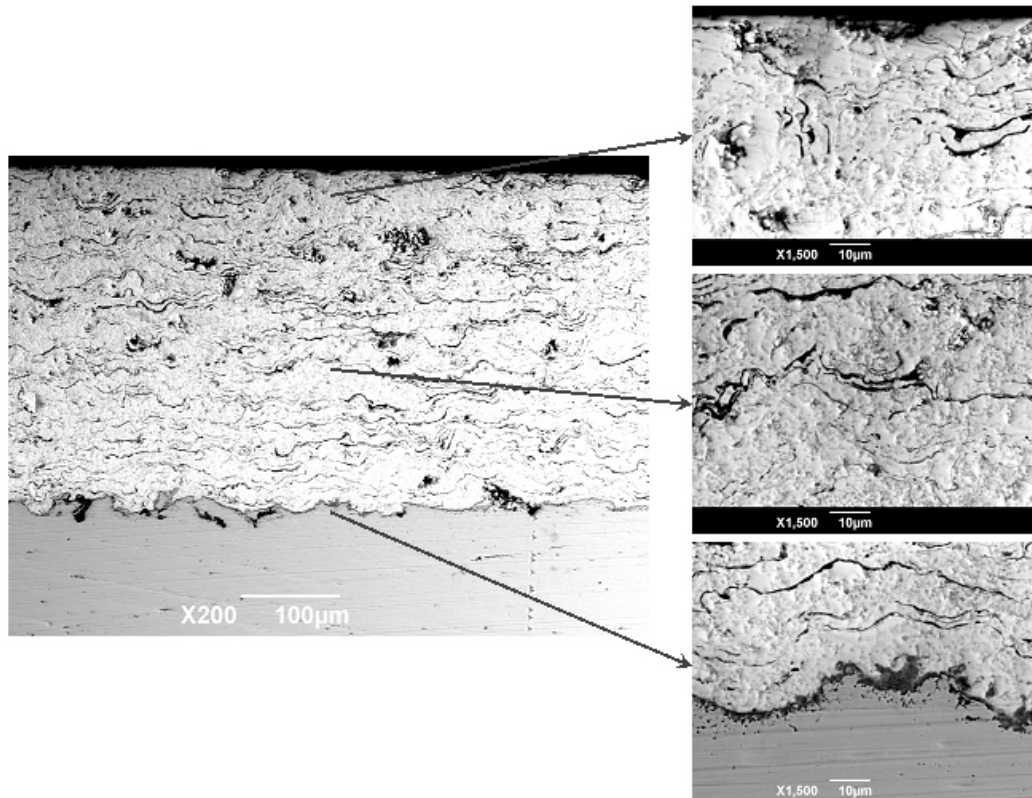


Figure 5. SEM-images of coatings from zirconium dioxide after annealing at 1000 ° C.

micro-discontinuities in the form of thin interlayers, the size of which is several tens of micrometers in length and 0.3-1.0  $\mu\text{m}$  in thickness. Thin layers are formed as a result of the spreading of molten particles of the sprayed metal over the surface. The results of X-ray microspectral analysis show that the formed coating is characterized by a more uniform distribution of all the chemical elements that make up the composition.

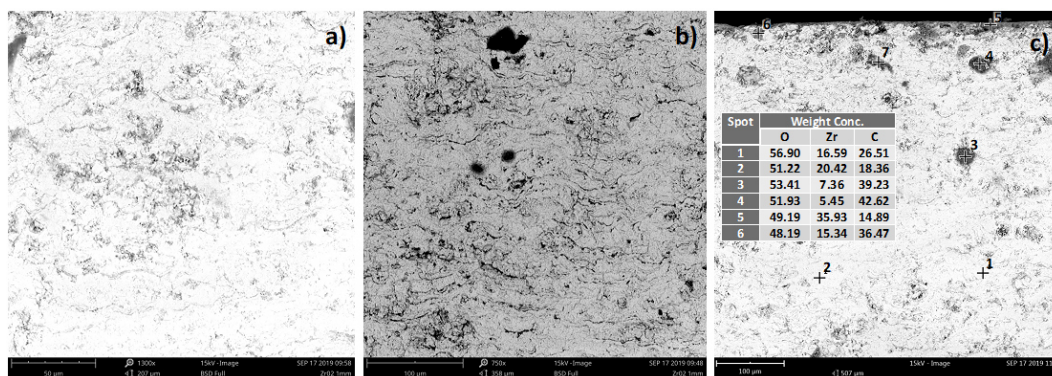


Figure 6. SEM-image of the surface (a), cross-section (b) of coatings of zirconium dioxide and the results of micro X-ray spectral analysis (c).

## Conclusion

1. The coatings of zirconium dioxide with a thickness of 360-370  $\mu\text{m}$  was obtained by the detonation method. It was determined that the coatings have pores and the average pore size is 5  $\mu\text{m}$  by metallographic analysis method.

2. Electronic microscopic analysis showed that the resulting coatings are characterized by the presence of high density and uniformity, as well as the presence of individual pores. Two groups of pores have been identified: round micro-discontinuities several micrometers in size and micro-discontinuities in the form of thin interlayers, the size of which is several tens of micrometers in length and 0.3-1.0  $\mu\text{m}$  in thickness. There is an increase in the number and size of micro-continuity in the form of thin layers after annealing.

3. X-ray diffraction analysis showed that the phase composition of coatings before and after annealing consists of  $t\text{-ZrO}_2$ . After annealing, there is an increase in the degree of  $t\text{-ZrO}_2$  tetragonality.

4. It was determined that the microhardness of zirconium dioxide coatings increases by 10-25% depending on the annealing temperature after annealing. The results of nanoindentation showed that the nanohardness of the coatings after annealing at 1000  $^\circ\text{C}$  increases on 50% and reached to 15.8 GPa.

5. Determined that increase the hardness of zirconium dioxide after annealing at 900-1100  $^\circ\text{C}$  is associated with a higher degree of tetragonality  $t\text{-ZrO}_2$  phase.

## Acknowledgments

This research is funded by the Science Committee of the Ministry of Education and Science of the Republic of Kazakhstan (Grant No. AP08957765).

## References

- [1] A. Sivkov et al., Surface and Coatings Technology **292** (2016) 63-71.
- [2] Wang Qun et al., International Journal of Refractory Metals and Hard Materials **81** (2019) 242-252.
- [3] D.K. Yeskermessov et al., Physics **88** (2017) 8-17.

- [4] J. Jayaraj et al., Corrosion Science **48** (2006) 950-964.
- [5] D.L. Alontseva et al., Physics **71** (2013) 4-11. (in Russian)
- [6] Niu Shaopeng et al., Surface and Coatings Technology **307(A)** (2016) 963-970.
- [7] M.M. Student et al., Materials Science **54** (2018) 22-29.
- [8] E. Kadyrov et al., J. Therm. Spray Technol. **3** (1995) 280-286.
- [9] X.M. Song et al., Surf. Coat. Tech. **270** (2015) 132-138.
- [10] Z.J. Fan et al., Surf. Coat. Tech. **277** (2015) 188-196.
- [11] V.Y. Ulianitsky et al., Advanced powder Technolog **29** (2018) 1859-1864.
- [12] M.M. Mikhailov et al., Surface & Coatings Technology **319** (2017) 70-75.
- [13] V.Y. Ulianitsky et al., Materials Letters **181** (2016) 127-131.
- [14] D.V. Dudina et al., Ceramics International **42** (2016) 690-696.
- [15] B.K. Rakhadilov et al., Key Engineering Materials **821** (2019) 301-306.
- [16] V.Y. Ulianitsky et al., Metals **12** (2019) 1244.
- [17] I.S. Batraev et al., Materials Today: Proceedings **4** (2017) 11346-11350.
- [18] D. Buitkenov et al., Eurasian Journal of Physics and Functional Materials **4(1)** (2020) 86-92.
- [19] D.V. Shtanskiy et al., Fizika tverdogo tela **48(7)** (2006) 1231-1238. (in Russian)
- [20] W.D. Nix et al., Thin Solid Films **515** (2007) 3152-3157.
- [21] Zhang Jia-Ping et al., Surface & Coatings Technology **285** (2016) 24-30.
- [22] G.Ia. Akimov et al., Fizika tverdogo tela – Solid state physics **11** (2005) 1978-1980. (in Russian)